Pretransitional diffuse neutron scattering in the mixed perovskite relaxor $K_{1-x}Li_xTaO_3$

Grace Yong and Jean Toulouse
Department of Physics, Lehigh University, Bethlehem, Pennsylvania 18015

Ross Erwin
NIST Center for Neutron Research, Building 235, Gaithersburg, Maryland 20899-0001

Stephen M. Shapiro
Department of Physics, Brookhaven National Laboratory, Building 510B, Upton, New York 11973-5000

Bernard Hennion
Laboratoire Léon Brillouin, CEA/Saclay 91191 GIF-sur-YVETTE Cedex, France
(Received 22 November 1999; revised manuscript received 15 May 2000)

Several previous studies of $K_{1-x}Li_xTaO_3$ (KLT) have revealed the presence, above the structural transition, of polar nanoregions. Recently, these have been shown to play an essential role in the relaxor behavior of KLT. In order to characterize these regions, we have performed a neutron-scattering study of KLT crystals with different lithium concentrations, both above and below the critical concentration. This study reveals the existence of diffuse scattering that appears upon formation of these regions. The rodlike distribution of the diffuse scattering along cubic directions indicates that the regions form in the shape of discs in the various cubic planes. From the width of the diffuse scattering we extract values for a correlation length or size of the regions as a function of temperature. Finally, on the basis of the reciprocal lattice points around which the diffuse scattering is most intense, we conclude that the regions have tetragonal symmetry. The large increase in Bragg intensities at the first-order transition suggests that the polar regions freeze to form large structural domains and the transition is triggered by the percolation of strain fields through the crystals.

I. INTRODUCTION

Relaxors constitute a very important family of ferroelectrics that is receiving growing attention because of the remarkable behavior of its members. Initially recognized for the significant frequency dispersion displayed by their dielectric constant,[1] they have also recently become the focus of a new research effort because of the unusually large strains they exhibit in single crystal form when subjected to modest external electric fields.[2,3] Although most of the known relaxors are lead compounds (PMN, PZT, etc.), $K_{1-x}Li_xTaO_3$ (KLT) has also been shown to be a relaxor.[4] In fact, because of its much greater simplicity, KLT now represents a model system for relaxors and one that can be used to understand the microscopic origin of the relaxor behavior.

The first feature that makes KLT a simple model system is that its parent compound, $KTaO_3$, is one of the few ternary perovskites that do not undergo a structural phase transition.[5,6] When doped with lithium above a critical concentration ($x_c = 2.2\%$), KLT undergoes a structural transition to a tetragonal phase.[7,8] The second feature is that K^+ is a simple ionic cation, compared to cations such as Pb^{2+} and Bi^{3+} found in other relaxors that form partially covalent bonds with oxygen. As a result, the latter do not sit at cubic symmetry sites and the local structure is therefore strongly distorted even at high temperatures.[9,10] Finally, the aliovalent doping required to induce relaxor behavior in relaxors such as PMN or PZT results in a charge imbalance that can only be corrected by chemical ordering while, in KLT, Li^+ substitutes isovalently for K^+, giving rise to the relaxor behavior without introducing vacancies, additional charges or chemical variations.

In $K_{1-x}Li_xTaO_3$, the small Li^+ substitutional ion goes off center in one of six [100] directions, thus forming an electric dipole. The most often quoted value of the lithium displacement is 1.26 Å (Ref. 11) although a value of 1.6 Å (Ref. 12) has also been reported. At high temperature, the lithium off-center reorients between six crystallographically equivalent orientations.[11] At lower temperatures, the orientations of nearby dipoles become correlated, leading to the formation of polar nanoregions.[11,13,14] In a recent study, one of us has shown that the relaxor behavior was in fact associated with the coupled reorientations of several lithium ions through 90° jumps.[15]

The existence of polar nanoregions in KLT is by now well established, based on several different dynamical measurements, dielectric spectroscopy, polarization hysteresis loops,[4] and Raman scattering.[14] The most direct evidence should, however, come from x-ray and neutron diffuse scattering, which probe structural distortions directly. Only one paper has reported observation of diffuse scattering in KLT, using x rays.[8] In a 1.6% ($x < x_c$) KLT sample, diffuse scattering was reported near the (013) reciprocal lattice points in the [010] direction, slowly rising with decreasing temperature and reaching a plateau below 40 K. In a 5.4% ($x > x_c$) KLT sample, diffuse scattering was reported around (013), going through a maximum at the transition and disappearing below. In the present paper we report the results of a comprehensive neutron-scattering study in which we have investigated diffuse scattering in KLT for three different concentrations,

around a number of reciprocal lattice points and in various directions. This study is complementary to the x-ray study described above because neutrons can probe the bulk crystal and give better energy resolution while x rays are restricted to a certain depth below the surface but give better spatial resolution. Before presenting the diffuse scattering results above the transition, it is, however, useful to review the low-temperature behavior of KLT for the different concentrations investigated. The nature of the low-temperature phase may indeed contain information on the distortions that are responsible for the diffuse scattering above the transition.

For very low concentrations ($x<x_{\text{critical}}=0.022$), KLT remains cubic at all temperatures, as does its parent compound $KTaO_3$.[7,8] For intermediate concentrations, KLT undergoes a transition from a cubic phase at high temperature to a tetragonal phase at low temperature. Amongst others, this was shown in a neutron study of acoustic phonons in a 3.5% sample with and without a bias electric field[16] and in an x-ray study of a 5.4% sample that reported a disordered polar phase with average tetragonal symmetry at low temperature.[8] At higher concentration ($\sim$12%), another study also reported a low temperature disordered phase but with triclinic symmetry.[17] According to Ref. 8, when 1.6% KLT is cooled below T_c without a bias field, large structurally ordered quadrupolar ''domains'' form, containing disk-shaped polar domains with lateral dimension greater than 1000 Å and an aspect ratio greater than 10. We note that, according to Raman data in 1.4 and 5.4 % KLT, this lateral dimension may even reach several thousands ($\sim$4000 Å).[18] In summary, the strong anisotropic static scattering, arising from clusters of frozen polarization below T_c, suggests the presence of dynamic precursors (polar nanoregions) above T_c.

II. EXPERIMENTAL

Crystals with different lithium concentrations (x) were studied using neutron scattering. They are listed in Table I, along with their transition temperatures T_c. For 6 and 13 %,

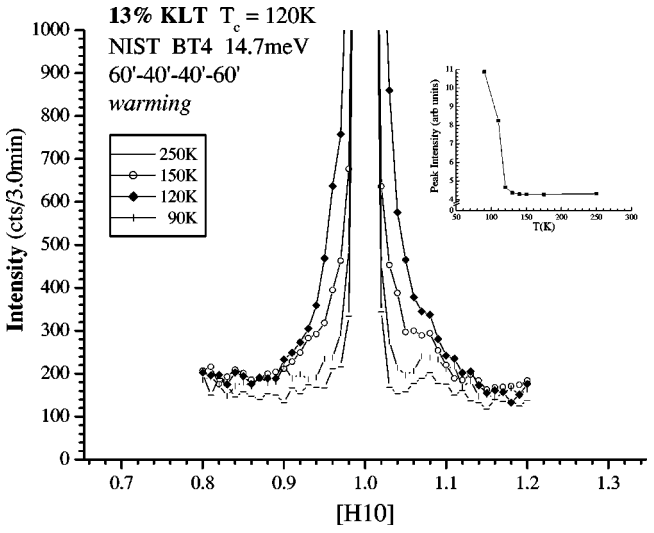

FIG. 1. Elastic scans at the (110) reciprocal point in the 13% KLT single crystal. Diffuse scattering is maximum at 120 K. The top-right inset also shows that the Bragg peak intensity increases rapidly below 120 K.

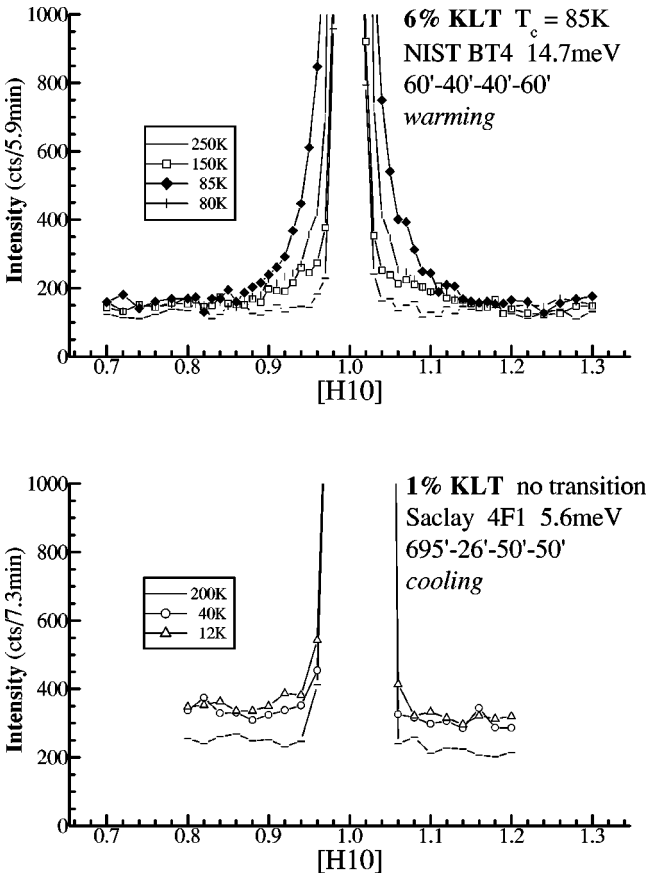

FIG. 2. Elastic scans at the (110) reciprocal point in 6 and 1 % KLT single crystals. As in the 13% KLT (Fig. 1), the diffuse scattering in the 6% KLT is maximum at 85 K, below which the Bragg intensity increases. The 1% KLT crystal did not display any diffuse scattering or increase of Bragg intensity but only an increase in background.

T_c is known from previous dielectric measurements. As shown in the present results, it coincides with the onset of extinction or decrease in magnitude of the (110) Bragg peak (upon warming) as well as with the maximum of the diffuse scattering.

The neutron measurements were performed at the National Institute of Standards and Technology (NIST) on the three triple axis spectrometers BT2, BT4, and BT9 and at Saclay (France) on the 4F1 spectrometer. The NIST spectrometers have a better spatial Q resolution for diffuse scattering while the Saclay spectrometer has better energy resolution for quasielastic scattering. The wavelengths used for the data displayed in this paper were 2.36 Å (14.7 meV) or 2.46 Å (13.5 meV) at NIST and 3.82 Å (5.6 meV) at Saclay.

The NIST BT2, BT4, and BT9 are conventional thermal

TABLE I. Dimensions, mosaicity, and transition temperatures of the KLT samples.

Conc.	Volume (mm^3)	Mass (g)	Mosaicity	T_c(K)
1%	7×5.5×4	1.0		no transition
6%	13×6×4.5	2.7	$3'\pm3'$	85
13%	8×7×5.5	2.2	$9.5'\pm1'$	120

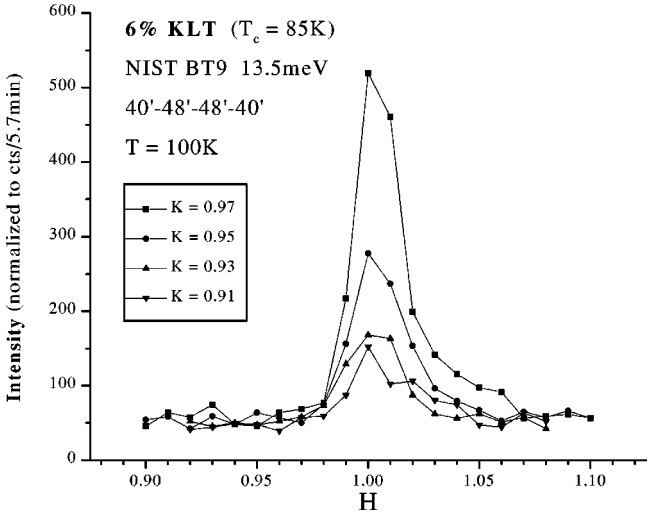

FIG. 3. Elastic scans near the (110) reciprocal point across the diffuse scattering ridge in the 6% KLT at 100 K.

neutron triple axis spectrometers with (002) pyrolytic graphite monochromator and analyzer. The Saclay 4F1 is a high-energy resolution triple axis spectrometer on a cold source. In the Saclay experiment, the first of the two parallel (002) pyrolytic graphite monochromators was vertically bent while the second was horizontally curved. The (002) pyrolytic graphite analyzer was flat for the (elastic) diffuse scattering in order to improve the q resolution in the plane but was curved for the quasielastic scattering (since curving the analyzer improves the energy resolution). Soller slits were not used and the geometry of the spectrometer gave natural collimations of $695'$-$26'$-$50'$-$50'$. A pyrolytic graphite filter was placed after the sample to minimize higher-order contaminations. Most of the data in this paper were obtained upon warming.

III. RESULTS

The diffuse-scattering measurements were made in the [001] and [110] zones, around many different reciprocal lattice points and in several directions. A typical scan is presented in Fig. 1, which reveals diffuse scattering around the (110) point in the [010] direction for the 13% KLT sample at different temperatures. The diffuse-scattering peak grows in intensity with decreasing temperature, reaching a maximum at the transition $T_c = 120$ K, and abruptly disappearing below. The finite correlation length at T_c and the sudden disappearance of the diffused scattering below are consistent with the first-order nature of the transition, which is also evident from dielectric measurements.[19,20] The inset of Fig. 1 shows the Bragg peak with a relatively constant magnitude down to 120 K and a rapid increase below. Figure 2 shows a similar behavior for the 6% KLT sample with a transition at $T_c = 85$ K but a very different behavior for the 1% KLT sample which does not exhibit a transition. For the latter sample, one observes only an increase in the flat background with decreasing temperature. Even for the two higher concentrations, which exhibit a phase transition, it is interesting to note that, while diffuse scattering is observed around certain reciprocal lattice points in certain directions, other directions only reveal a similar increase in the flat background. This observation indicates that, in the latter directions, there is no particular order of the polarization or atomic displacements and, consequently, no particular Q dependence. Scans at different values of Q in the [010] direction are shown in Fig. 3 and reveal diffuse scattering that is restricted to relatively narrow ridges along cubic directions. The overall diffuse scattering distribution around the (110) and (111) reciprocal lattice points is mapped out in Fig. 4 and reflects, as it should, the *average* cubic symmetry of the crystal. Energy scans of the diffuse scattering were also performed at the reciprocal point (0.93, 1, 0) at 100 and 300 K. At both temperatures the elastic peak centered at zero energy only had the width of the resolution. Thus, as far as the neutron measurements are concerned, the diffuse scattering is static in character. This is also consistent with the dielectric loss results, which locate the relaxor peak in the kHz to MHz frequency range at these temperatures.[4] These frequencies fall well inside the energy resolution of the neutron spectrometer.

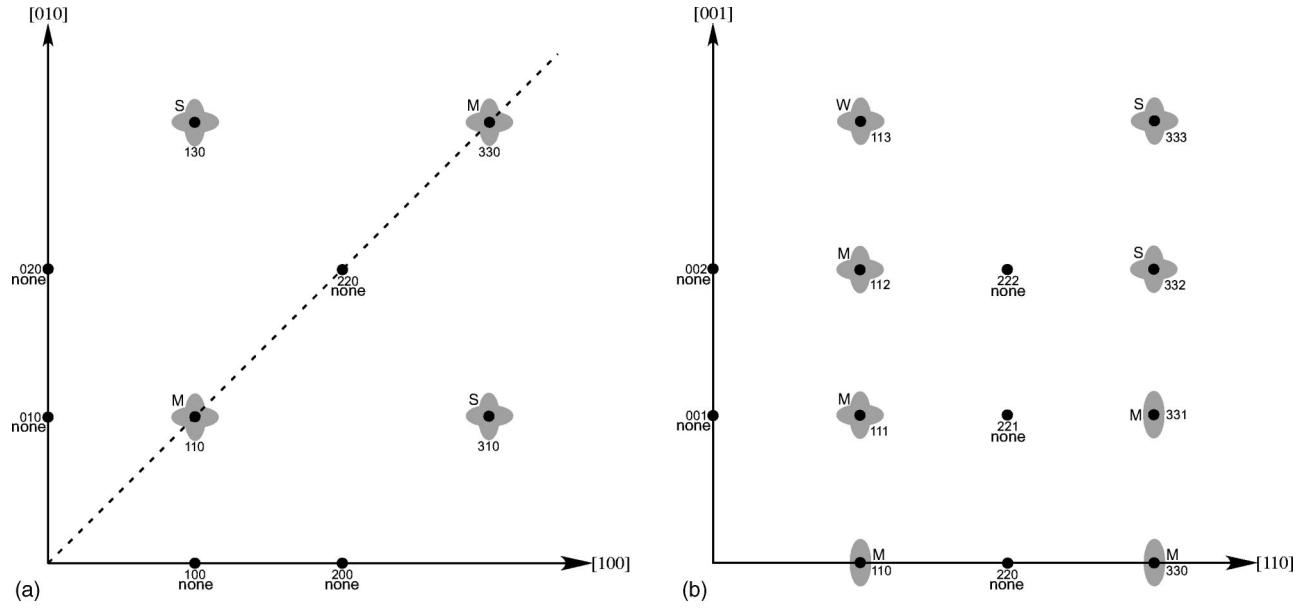

FIG. 4. Map of the diffuse scattering in the 13% KLT at $T = T_c = 120$ K (a) [010][100] and (b) [001][110] scattering planes.

IV. ANALYSIS AND DISCUSSION

We first summarize the observations made on KLT in the present experiments.

(i) Diffuse scattering appears at temperatures well above the transition, the latter being marked by relief of extinction or a sharp increase in the magnitude of the Bragg peak.

(ii) Diffuse scattering takes the form of ridges extended along [00l]-type directions in reciprocal space.

(iii) Diffuse scattering is found around reciprocal lattice points that have at least two or three odd indices.

In agreement with the results of other measurements mentioned in the Introduction, the diffuse scattering reported here provides direct evidence for the presence of polar regions or, more exactly, for the atomic displacements associated with them. The present results contain three different types of information which we examine next. (1) The direction of the diffuse scattering reveals the orientation of these regions.

(2) The width in Q of the diffuse scattering shows that these regions have a finite size; as we show below, their size (correlation length) can be obtained from the full width at half maximum (FWHM) of the diffuse-scattering peak.

(3)The set of reciprocal lattice points around which diffuse scattering is observed contains information on the symmetry of the lattice distortions.

We first look at the geometry of the diffuse scattering. The diffuse scattering is in the form of rods extended along cubic directions. Based on elementary diffraction considerations,[21] such an intensity distribution indicates that the polar regions have the shape of flat disks. Within the plane of the disk, the ferroelectric displacements are correlated over short distances. The correlation length is therefore much longer along two of the axes than along the third. Past measurements have shown that, in KLT, the Li ions are displaced along [100] directions, which are also the directions of the ferroelectric displacements of the host ions in the perovskite structure (see Table II). On that basis, the model presented below assumes such displacements within the polar regions. These displacements will be correlated in two directions and random in the third. The fact that the disorder comes from a random modulation of the displacements along a direction perpendicular to the main symmetry axis of the regions explains that no diffuse scattering is found around [00l] Bragg peaks.

TABLE II. Correlation lengths ξ measured by other workers in KLT (no applied electric field).

Sample	$T<T_c$	$T=T_c$	$T>T_c$
Dielectric measurement			
Pure KTa [a]			15 Å (0 K)
Asymmetry of Raman TO_1 peak			
Pure KT [b]			16 Å (2 K), 6 Å (100 K)
1.6% KLT [c]			100 Å (15 K), 20 Å (80 K)
Asymmetry of Raman TO_2 peak			
1% KLT [d]			33 Å (4–10 K)
3.5% KLT [d]	36 Å (4 K)	36 Å (55 K)	
10% KLT [d]	40 Å (4 K)	40 Å (80 K)	
Second harmonic generation			
1.6% KLT [e]			60 Å (20 K), 55 Å (36 K)
2.6% KLT [e]	105 Å (20 K)	100 Å (48 K)	
3.4% KLT [e]	120 Å (20 K)	115 Å (53 K)	
6% KLT [e]	230 Å (30 K)	175 Å (86 K)	
pure KT [f]			16 Å (4 K)
3.6% KLT [g]	2000 Å (40 K)		
6.3% KLT [g]	10 000 Å (40 K)		
0.8% KLT [h]			120 Å (20 K)
1.6% KLT [h]			140 Å (20 K)
2.2% KLT [h]	570 Å (20 K)		
3.6% KLT [h]	1400 Å (20 K)		
4.3% KLT [h]	7000 Å (20 K)		
6.3% KLT [h]	$\geqslant$28 000 Å (20 K)		
Second harmonic generation and linear birefringence			
1.6% KLT [i]			80 Å (10–55 K)
Hyper-Rayleigh scattering			
Pure KT [a]			18 Å (10 K), 5 Å (200 K)
Hyper-Raman scattering			
1.1% KLT [k]			40 Å (0 K)
1.6% KLT [k]			50 Å (0 K)
3.6% KLT [k]	150 Å (0 K)		

TABLE II. (*Continued*).

Sample	$T<T_c$	$T=T_c$	$T>T_c$
Microwave-induced Brillouin scattering			
1.1% KLT [l]			$\xi<100$ Å (15–36 K)
2.6% KLT [l]	$\xi<100$ Å ($T<50$ K)		$\xi<100$ Å ($T>100$ K)
6.3% KLT [l]	$\xi<100$ Å ($T<85$ K)		$\xi<100$ Å ($T>100$ K)
X-ray diffuse scattering			
1.6% KLT [m]			$\xi>100$ Å ($T\sim10$ K)
Neutron TO_1 phonon dispersion curve			
Pure KT [n]			9 Å (15 K), 4 Å (90 K)
Pure KT [o]			15 Å (4 K), 8 Å (77 K)

[a]M. Maglione, Ferroelectrics, **137** 113 (1992); M. Maglione, S. Rod, and U. T. Hochli, Europhys. Lett. **4**, 631 (1987).
[b]H. Uwe, K. B. Lyons, H. L. Carter, and P. A. Fleury, Phys. Rev **33**, 6436 (1986).
[c]G. P. Banfi, P. Calvi, P. Camagni, E. Giulotto, and G. Samoggia, *Proceedings of the International Conference on Defects in Insulating Materials*, edited by O. Kanert and J. M. Spaeth (World Scientific, Singapore, 1993), Vol. 1, p. 660.
[d]P. DiAntonio, B. E. Vugmeister, J. Toulouse, and L. A. Boatner, Phys. Rev **47**, 5629 (1993); P. DiAntonio, Ph.D. thesis, Lehigh University 1994.
[e]G. A. Azzini, G. P. Banfi, E. Giulotto, and U. T. Hochli, Phys. Rev **43**, 7473 (1991); G. A. Azzini, G. P. Banfi, E. Giulotto, G. Samoggia, and U. T. Hochli, ECOOSA 90–*Quantum Optics. Proceedings of the European Conference on Optics, Optical Systems and Applications* (IOP, Bristol, 1991), p. 195; G.P.;Banfi, P. Camagni, E. Giulotto, G. Samoggia, and U. T. Hochli, Ferroelectrics **124**, 133 (1991).
[f]W. Prusseit-Elffroth and F. Schwabl, Appl. Phys. **51**, 361 (1990).
[g]P. Voigt, K. Betzler, N. Schmidt, and S. Kapphan, Ferroelectrics **106**, 149 (1990).
[h]P. Voigt and S. Kapphan, Ferroelectrics **157**, 239 (1994); P. Voigt and S. Kapphan, J. Phys. Chem. Solids **55**, 853 (1994); P. Voigt, S. Kapphan, L. Oliveira, and M. S. Liu, Rad. Eff. Defects Solids **134**, 229 (1995).
[i]G. P. Banfi, P. Calvi, and E. Giulotto Phys. Rev. B **51**, 6231 (1995).
[j]H. Vogt, Phys. Rev. B **41**, 1184 (1990); H. Vogt, Ferroelectrics **107**, 79 (1990).
[k]H. Vogt J. Phys: Condens. Matter **7**, 5913 (1995).
[l]M. Lehndorff, Ph.D. thesis, Universitat Konstanz, 1986; M. Lehndorff and K. Dransfeld, Verh. Deutsch. Phys. Ges. **21**, 1063 (1986); D. Sommer, W. Kleemann, M. Lehndorff, and K. Dransfeld, Solid State Commun. **72**, 731 (1989).
[m]S. R. Andrews, J. Phys. C **18**, 1357 (1985).
[n]S. Rod and J. J. van der Klink, Phys. Rev. **49**, 15 470 (1994).
[o]L. Foussadier, M. D. Fontana, and W. Kress, J. Phys.: Condens. Matter **8**, 1135 (1996).

Next, we estimate the size or correlation length of these regions. Following the above explanation, it is important to recall that the direction in which the diffuse scattering is more extended corresponds to the shorter dimension of the regions and vice versa. Because the diffuse intensity is more extended along the ridge, the shorter correlation length can be measured more accurately than the longer one. In order to evaluate the correlation length of the displacements, i.e., the size of the polar regions, the diffuse-scattering peaks in both directions (along the ridge and perpendicular to it) were fitted with Lorentzian functions (see Fig. 5 along the ridge). The parameters from the fits, intensity and FWHM corresponding to the shorter correlation length are plotted in Fig. 6 for the 6 and the 13 % samples as a function of temperature. At T_c, the diffuse scattering reaches maximum intensity and its width a minimum, corresponding to a maximum but finite value of the correlation length. The nondivergence of the correlation length, is consistent with a first-order transition.[22] It is particularly interesting to note that the maximum correlation length for the 6% KLT sample, ~46 Å near $T_c=85$ K, is only slightly longer than the maximum correlation length for the 13% KLT sample, ~30 Å at $T_c=120$ K. This observation suggests a percolation type of transition[23] in which, when the distorted regions reach a certain threshold size (~40 Å), a strain-driven transition occurs[24] that freezes the polar regions in an antiferroelectriclike arrangement. When cooled in the absence of an external field, the low-temperature structure of KLT is in fact known to be tetragonal but without a net spontaneous polarization.[25] The slightly shorter correlation length in the

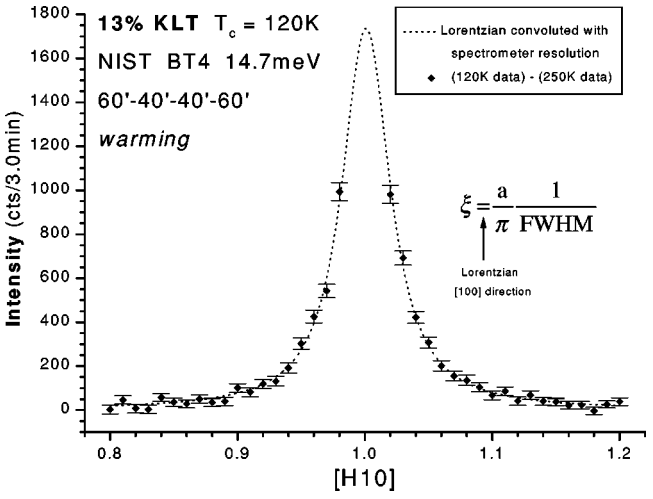

FIG. 5. Fit to the diffuse scattering at 120 K in the 13% KLT by a Lorentzian convoluted with the spectrometer resolution function. Note that the middle high data points corresponding to the Bragg contribution have been removed.

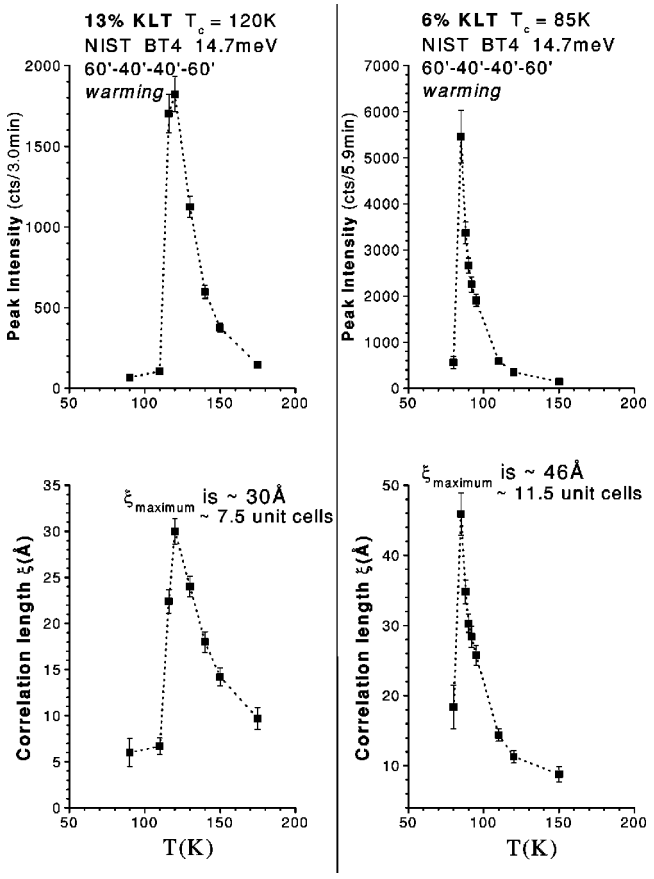

FIG. 6. Intensity of the diffuse scattering and correlation length obtained from the fits shown in Fig. 5 for the 13 and 6 % KLT samples.

13% sample may be a result of increased strain at higher concentrations. The longer correlation length, or diameter of the polar regions was similarly estimated. For the 6% crystal, the longer correlation length is found to be $\sim 3-4$ times greater than the shorter correlation length at 150 K but only $\sim 2-3$ times greater than the shorter one at 100 K. This result would seem to indicate that the polar regions first form as very flat disks, which then become larger but also fatter as the temperature decreases. Comparing diffuse-scattering intensities while taking into account differences in sample weight and monitor, the peak values of the Lorentzian curves are found to be comparable for the two concentrations 6 and 13 %. This result suggests that the volume fraction of the crystal that is transformed is approximately the same for the two concentrations. This is consistent with the observation of similar correlation lengths at the transition for those two concentrations.

Finally, we examine the information contained in the particular set of reciprocal lattice points around which diffuse scattering is observed, with at least two odd indices, and show that the results are compatible with a tetragonal distortion of the lattice in the nanoregions. This is obviously quite consistent with the fact that all the displacements are expected to be along [100] directions leading to the known low-temperature tetragonal phase. For the sake of argument, in the following model, we assume that the neutron beam is incident along y (b axis of the crystal) on a flat disk (polar region) with its polar axis in the $z(c)$ direction, i.e., extended ferroelectric correlations in the y and z (b and c) directions and its short dimension along the x (a) direction. The scattering plane is therefore the a-b plane. Equivalently, we could have chosen the same polar regions with their polar axis along y but still in the y-z plane or regions in the x-y plane with their polar axis along either x or y. The elastic site-averaged scattering function is

$$S_{\text{elastic}}(\vec{Q}) = \left| \sum_c \sum_d \langle b_{c,d} \rangle e^{(i\vec{Q}\cdot\vec{r}_c)} e^{(i\vec{Q}\cdot\vec{r}_d)} \right|^2, \qquad (1)$$

where $\langle b \rangle$ is the neutron-scattering length of a given element in the unit cell and the sums are over unit cell positions $\vec{r}_c$ and atoms $\vec{r}_d$ in the unit cell and $\vec{Q} = h\hat{a}^* + k\hat{b}^* + l\hat{c}^*$, where $\hat{a}^*$, $\hat{b}^*$, and $\hat{c}^*$ are unit vectors in reciprocal space and h,k,l are integers. Along the x axis, short dimension of the disk, the model considers a random sequence of up and down polarization regions on an otherwise perfect lattice. We fix the region size along the x axis at N times the length of the unit cell. This corresponds to a well-known case of disorder for which the diffuse-scattering function is given by[21]

$$S_{\text{diff}}(\vec{Q}) = CS(Q_x) \left| \sum_d \langle b_d \rangle e^{(i\vec{Q}\cdot\vec{r}_{d0})} \sin(2\pi l \delta_d) \right|^2, \qquad (2)$$

where $\delta_{\mathbf{d}}$ is the fractional unit cell displacement along the c axis of the atom that has an undisplaced position $\vec{r}_{d0}$ with respect to the origin of the unit cell. Again we have taken the ferroelectric displacements δ all to be in the z direction and are considering flat polar regions with their short dimensions along x. The diffuse scattering arises from variations of the phase sum in Eq. (1) from its average due to the lack of long-range correlation of the local polarization or atomic displacements along the x direction. This produces the sine function term in Eq. (2). The diffraction of many superposed neutron waves lead to the following expression for $S(Q_x)$:

$$S(Q_x) = \frac{\sin^2(NQ_x a/2)}{\sin^2(Q_x a/2)}. \qquad (3)$$

The width of this function along Q_x is approximately $2\pi/Na$ where N is the number of unit cells along the x axis and a is the unit cell parameter along the uncorrelated direction. Now, the sum over all the unit cells in the formula for the diffuse scattering, Eq. (2), can be written

$$\begin{aligned} F(h,k,l) = {} & b_K(1-c_{\text{Li}})\sin(2\pi l \delta_K) + b_{\text{Li}} c_{\text{Li}} \sin(2\pi l \delta_{\text{Li}}) \\ & + b_{\text{Ta}}(-1)^{h+k+l}\sin(2\pi l \delta_{\text{Ta}}) \\ & + b_{\text{O}}(-1)^{h+k}\sin(2\pi l \delta_{\text{O1}}) + b_{\text{O}}(-1)^l \\ & \times [(-1)^h + (-1)^k]\sin(2\pi l \delta_{\text{O2}}), \end{aligned}$$

where c_{Li} is the site diffraction occupancy of the Li atom. The O_1 (apex) oxygen site is at (1/2,1/2,0) along the z axis (displacement axis) while O_2 and O_3 are the remaining two equivalent oxygens in the unit cell. There are four different types of $F(h,k,l)$ based on the parity of h, k, and l. Using the small displacement approximation for all of the atoms except lithium, and factoring out $2\pi l$, the values of $F(h,k,l)$ become

$$F(h_o,k_o,l_o)=f_{\mathrm{Li}}(l)+(1-c_{\mathrm{Li}})b_{\mathrm{K}}\delta_{\mathrm{K}}-b_{\mathrm{Ta}}\delta_{\mathrm{Ta}}+b_{\mathrm{O}}(\delta_{\mathrm{O1}}+2\delta_{\mathrm{O2}}), \quad (4)$$

$$F(h_o,k_o,l_e)=f_{\mathrm{Li}}(l)+(1-c_{\mathrm{Li}})b_{\mathrm{K}}\delta_{\mathrm{K}}+b_{\mathrm{Ta}}\delta_{\mathrm{Ta}}+b_{\mathrm{O}}(\delta_{\mathrm{O1}}-2\delta_{\mathrm{O2}}), \quad (5)$$

$$F(h_o,k_e,l_o)=f_{\mathrm{Li}}(l)+(1-c_{\mathrm{Li}})b_{\mathrm{K}}\delta_{\mathrm{K}}+b_{\mathrm{Ta}}\delta_{\mathrm{Ta}}-b_{\mathrm{O}}\delta_{\mathrm{O1}}, \quad (6)$$

$$F(h_o,k_e,l_e)=f_{\mathrm{Li}}(l)+(1-c_{\mathrm{Li}})b_{\mathrm{K}}\delta_{\mathrm{K}}-b_{\mathrm{Ta}}\delta_{\mathrm{Ta}}-b_{\mathrm{O}}\delta_{\mathrm{O1}}, \quad (7)$$

$$F(h_e,k_e,l_o)=f_{\mathrm{Li}}(l)+(1-c_{\mathrm{Li}})b_{\mathrm{K}}\delta_{\mathrm{K}}-b_{\mathrm{Ta}}\delta_{\mathrm{Ta}}+b_{\mathrm{O}}(\delta_{\mathrm{O1}}-2\delta_{\mathrm{O2}}), \quad (8)$$

$$F(h_e,k_e,l_e)=f_{\mathrm{Li}}(l)+(1-c_{\mathrm{Li}})b_{\mathrm{K}}\delta_{\mathrm{K}}+b_{\mathrm{Ta}}\delta_{\mathrm{Ta}}+b_{\mathrm{O}}(\delta_{\mathrm{O1}}+2\delta_{\mathrm{O2}}), \quad (9)$$

where the subscripts e and o stand for even and odd, respectively, and where

$$f_{\mathrm{Li}}=c_{\mathrm{Li}}b_{\mathrm{Li}}\frac{\sin(2\pi l\delta_{\mathrm{Li}})}{2\pi l}. \quad (10)$$

As mentioned earlier, the ferroelectric displacements δ in the perovskite structure are opposite for the positive central ion and the six negatively charged oxygen ions. According to the model just presented, the Li-induced displacements giving rise to diffuse scattering should therefore be those corresponding to the equations above that have opposite signs for the contribution of the positive and negative ions, e.g., Eqs. (4) and (5). On the contrary, one would not expect diffuse scattering at reciprocal lattice points corresponding to Eqs. (7) and (9). For the other cases, diffuse scattering should be intermediate. This is indeed in agreement with the experiments: the strongest diffuse scattering is observed around points with at least two odd indices and no diffuse scattering is observed around points with only one odd index or all even indices (see Fig. 4).

Going into more detail, one might expect somewhat stronger diffuse scattering in cases corresponding to Eq. (4) since the two oxygen terms contribute with the same sign while, in the case corresponding to Eq. (5), the two oxygen terms contribute with opposite signs. However, the experiment indicated stronger diffuse scattering around (110) than around (331) and (113) and around (331) stronger (or possibly broader) in the $\langle 001\rangle$ direction than in the $\langle 110\rangle$ direction. This is probably due to the fact that lower index planes contain a higher density of atoms. It may also be related to the presence of striations sometimes visible in these crystals. In order to elucidate this point fully, a quantitative analysis of the diffuse scattering around several reciprocal lattice points would be needed. It is also interesting to note that, if δ_{Li} is 1/4, then the lithium term vanishes for all even l. With a Li displacement of approximately 1.2 Å and a lattice parameter of 3.998 Å, this condition is in fact close to being fulfilled. This further explains the absence of any diffuse scattering around the (002), (022), (222), and (004) Bragg peaks, already predicted to be weak by Eq. (9).

In the model presented above, the displacements of the host ions have been assumed to be the ferroelectric displacements corresponding to the soft transverse phonon mode and the displacement of the lithium ion to be along cubic directions. From previous studies and from the present work, it is now well established that the primary displacement of the lithium ions in KLT is along [100]. It is of course possible that there may be a small additional displacement along a second direction, most likely another [100] direction, such as $\langle 010\rangle$, resulting in a local orthorhombic symmetry. However, such a distortion has so far not been reported by anyone.

The model presented above reproduces qualitatively well the observed diffuse scattering, which therefore provides direct evidence for the presence, above the transition, of polar nanoregions with tetragonal symmetry. The strain fields associated with these regions must, however, remain relatively weak since no broadening of the Bragg peaks is observed. Upon passing through the transition temperature, a very significant increase in the Bragg intensities may signal either the development of very large strain fields (relief of extinction) or the freezing of finite size clusters. In his detailed and comparative x-ray study of KLT and KTN, Andrews concluded with the latter explanation. The experimental evidence in support of his conclusion is (i) that the structural changes taking place at the transition are very small ($c/a \sim 1.0014$ in 5% KLT) and should not generate large strain fields and (ii) that the integrated intensities of the Bragg peaks are found to be proportional in two very different crystals, 1.7% KTN and 5% KLT. Our results suggest a similar explanation. As can be seen in Fig. 1 the (110) Bragg peak does not show any broadening below T_c, despite a very large increase in intensity. This would rule out the strain or relief of extinction explanation and favor the frozen cluster one. This interpretation is also supported by the sudden drop in dielectric constant[15] and by the sudden increase in the nonpolar TO_3 phonon mode at the transition.[14]

The emerging model for the transition is the following. Above the transition, the polar regions are able to reorient between their various possible $\langle 100\rangle$ orientations, albeit more and more slowly as the transition is approached. The transition then corresponds to a freezing of the polar regions in fixed orientations. However, as indicated in the introduction, previous experimental studies have clearly shown that (1) the low-temperature phase is tetragonal and (2) in the absence of an external field, KLT does not exhibit any spontaneous polarization. The large increase in Bragg intensity through the transition can therefore be attributed to the freezing of the polar regions within structural domains such that, within a given domain, their polar axes are randomly distributed between two opposite directions along the tetragonal axis (antiferroelectriclike arrangement), both orientations giving rise to the same distortion. This would explain the absence of a net macroscopic strain or broadening of the Bragg peaks below the transition.

V. CONCLUSIONS

In the present report, we have presented diffuse-scattering results obtained on KLT crystals covering a wide range of concentrations from below critical to concentrated. For concentrations greater than critical, diffuse scattering is observed

above T_c around reciprocal lattice points with odd-odd-even and odd-odd-odd indices and in cubic directions. As shown by a microscopic model involving modulation of the polarization-atomic displacements, this indicates the presence of transformed regions with tetragonal symmetry. These regions have the shape of flat disks lying in cubic planes with their shorter dimension reaching 30–50 Å at T_c and, in a 6% crystal, the longer dimension being approximately ~ 3 times larger than the short one. Higher concentrations of lithium seem to slightly reduce the correlation length, possibly because of increased strain. The intensity of the diffuse scattering is also found to be the roughly the same in the 6 and 13 % at T_c. The transition is accompanied by a large increase in elastic scattering, which likely corresponds to the orientational freezing of polar regions into in an antiferroelectric arrangement within structural domains.

ACKNOWLEDGMENTS

We gratefully acknowledge L. A. Boatner for providing the KLT single crystals. This work was supported in parts by NSF Grant No. DMR 96-24436 and ONR Grant No. N00014-93-1-1100.

[1] G.A. Smolensky and A.I. Agranovskaya, Sov. Phys. Solid State **1**, 1429 (1960).
[2] S.E. Park and T.R. Shrout, J. Appl. Phys. **82**, 1804 (1997).
[3] J. Kuwata, K. Uchino, and S. Nomura, Ferroelectrics **37**, 579 (1981).
[4] J. Toulouse, B.E. Vugmeister, and R. Pattnaik, Phys. Rev. Lett. **73**, 3467 (1994).
[5] S.H. Wemple, Phys. Rev. **137**, A1575 (1965).
[6] J.P. Poirier, S. Beauchesne, and F. Guyot, in *Perovskite: A Structure of Great Interest to Geophysics and Materials Science*, edited by A. Navrotsky and D.J. Weidner (American Geophysical Union, Washington, D.C., 1989), p. 119.
[7] W. Kleemann, S. Kütz, and D. Rytz, Europhys. Lett. **4**, 239 (1987).
[8] S.R. Andrews, J. Chem. Phys. **18**, 1357 (1985).
[9] S. Teslic and T. Egami, Acta Crystallogr., Sect. B: Struct. Sci. **54**, 750 (1998); Ferroelectrics **222**, 163 (1999).
[10] J. Goodenough and J. M. Longo, in *Magnetic and Other Properties of Oxides and Related Compounds*, edited by K. Hellwege, Landolt-Bornstein, New Series, Group III, Vol 4, Part a (Springer-Verlag, Berlin, 1970), p. 144.
[11] J.J. van der Klink, D. Rytz, F. Borsa, and U.T. Höchli, Phys. Rev. B **27**, 89 (1983).
[12] E.A. Zhurova, V.E. Zavodnik, S.A. Ivanov, P.P. Syrnikov, and V.G. Tsirelson, Z. Naturforsch. **48**, 25 (1993); Russ. J. Inorg. Chem. **37**, 1240 (1992).
[13] M. Maglione, S. Rod, and U.T. Höchli, Europhys. Lett. **4**, 631 (1987).
[14] P. DiAntonio, B.E. Vugmeister, J. Toulouse, and L.A. Boatner, Phys. Rev. B **47**, 5629 (1993).
[15] R. Pattnaik and J. Toulouse, Ferroelectrics **222**, 367 (1999).
[16] J. Toulouse and B. Hennion, Phys. Rev. B **49**, 1503 (1994).
[17] S.A. Ivanov, V.V. Zhurov, G. Hermeler, and W. Depmeier, Mater. Sci. Forum **228-331**, 633 (1996).
[18] R.L. Prater, L.L. Chase, and L.A. Boatner, Phys. Rev. B **23**, 5904 (1981).
[19] P. Doussineau, Y. Farssi, C. Frènois, A. Levelut, K. McEnaney, J. Toulouse, and S. Ziolkiewicz, Europhys. Lett. **24**, 415 (1993).
[20] J. Toulouse and R. Pattnaik, J. Korean Phys. Soc. **32**, S942 (1998).
[21] S. Hendricks and E. Teller, J. Chem. Phys. **10**, 147 (1942).
[22] P. Pfeuty *et al.*, in *Introduction to the Renormalization Group and to Critical Phenomena* (Wiley, New York, 1977), pp. 5,6.
[23] J.A. Mydosh and G.J. Nieuwenhuys, in *Ferromagnetic Materials*, edited by E.P. Wohlfarth (North-Holland, Amsterdam, 1980), Vol. 1, p. 71.
[24] S. Rod and J.J. van der Klink, Phys. Rev. B **49**, 15 470 (1994); S. Rod, Ph.D. thesis, EPFL, Lausanne, Switzerland, 1991.
[25] U.T. Hochli, H.E. Weibel, and L.A. Boatner, J. Phys. C **12**, L563 (1979).